Science Advances
AAAS

advances.sciencemag.org/cgi/content/full/5/11/eaaw9807/DC1

Supplementary Materials for

The post-PAM interaction of RNA-guided spCas9 with DNA dictates its target binding and dissociation

Qian Zhang, Fengcai Wen, Siqi Zhang, Jiachuan Jin, Lulu Bi, Ying Lu, Ming Li, Xu-Guang Xi, Xingxu Huang, Bin Shen*, Bo Sun*

*Corresponding author. Email: sunbo@shanghaitech.edu.cn (B.Su.); binshen@njmu.edu.cn (B.Sh.)

Published 13 November 2019, *Sci. Adv.* **5**, eaaw9807 (2019)
DOI: 10.1126/sciadv.aaw9807

This PDF file includes:

SUPPLEMENTARY FIGURES

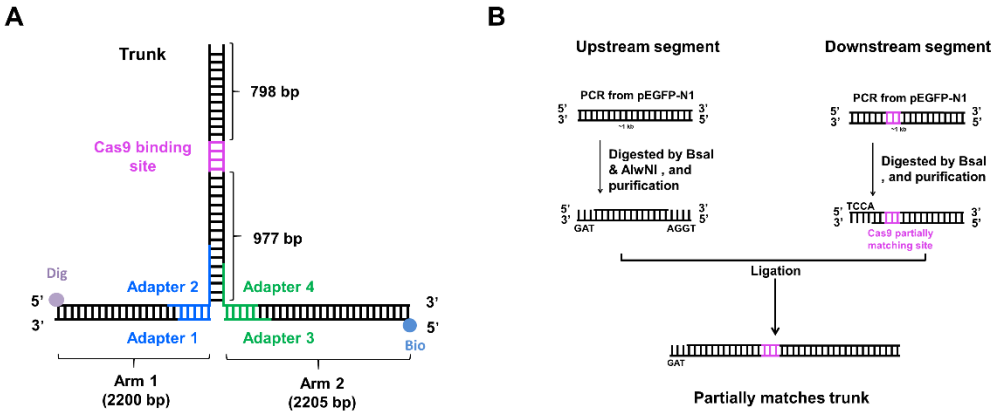

Fig. S1. DNA template design for single-molecule unzipping assay. (**A**) The DNA construct was made from three DNA segments: two arms and a trunk, linked through four short adapters (Methods and table S2). The trunk contains a single Cas9 binding site (purple). Two arms of the DNA construct were attached to a trapped microsphere and a microscope coverslip respectively. Unzipping of the trunk DNA was initiated from the fork due to a gap between adapters 1 and 3. (**B**) For trunks containing partially matched DNA target site, they were ligation products of two DNA segments: upstream segment and downstream segment (see Methods). The sequences of specific sites were modified by varying the forward primer sequence for the downstream segments.

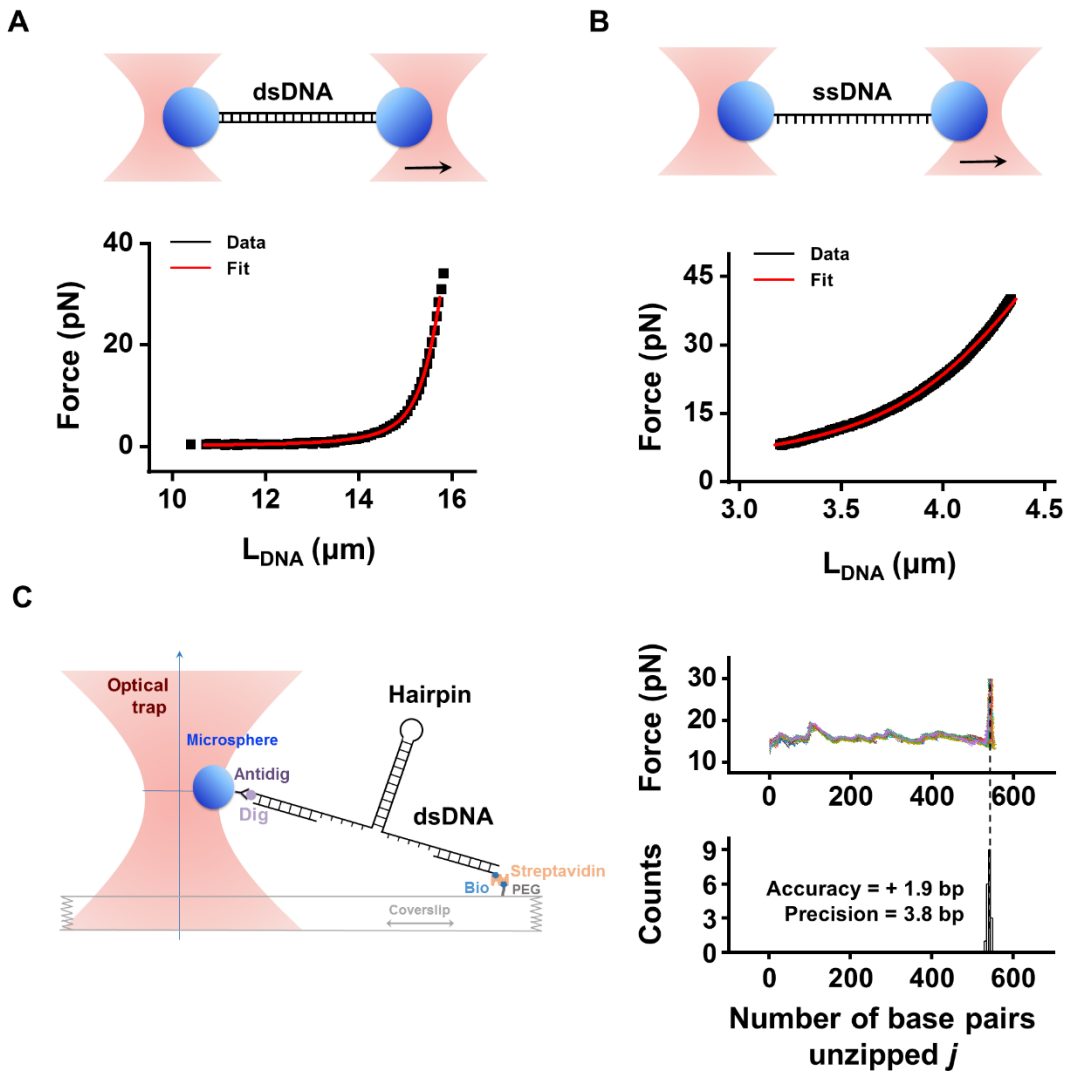

Fig. S2. Characterization of the DNA elasticity parameters and the accuracy and precision of the unzipping method. To determine dsDNA and ssDNA's elasticity parameters, we used duel optical tweezers and specific labeled DNA templates to measure the force-extension curves. For dsDNA, lambda DNA (48.5 kbp) was used (**A**). The force-extension relation of dsDNA was described using a modified Marko Siggia worm-like-chain (WLC) model (*39*): the contour length per base was 0.338 nm, the persistence length of DNA was 38.7 nm and the stretch modulus was 1,868 pN. For ssDNA, the short dsDNA (8.3 kbp) was labeled biotins on both ends of the same strand and was overstretched to achieve the ssDNA. The force-extension relation of ssDNA was described using an extensible freely jointed chain (FJC) model (*40*) in the force region between 8 pN and 40 pN (**B**): a counter length per base was 0.54 nm, Kuhn length was 1.50 nm and a stretch modulus was 338 pN. To characterize the ability of our unzipping technique to locate the absolute position of an interaction, we unzipped a 540 bp DNA template capped with a hairpin at the distal end and analyzed the measured location of the hairpin (**C**). A histogram was generated from the data points in the vertically rising section only. The measured hairpin location of the template was taken as the mean of

the histogram. The accuracy was determined by the difference between the mean of the histogram and the expected value (dashed vertical line). The precision was determined by the standard deviation of the histogram.

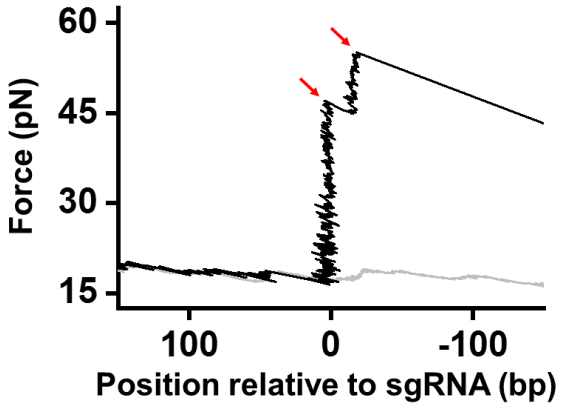

Fig. S3. A representative unzipping trace of on-target dCas9 with two peaks. A representative trace of forward DNA unzipping of an on-target dCas9 showed two peaks at the target site (indicated by red arrows). This two-peak unzipping feature occurred rarely for on-target dCas9 (15 out of 104 traces).

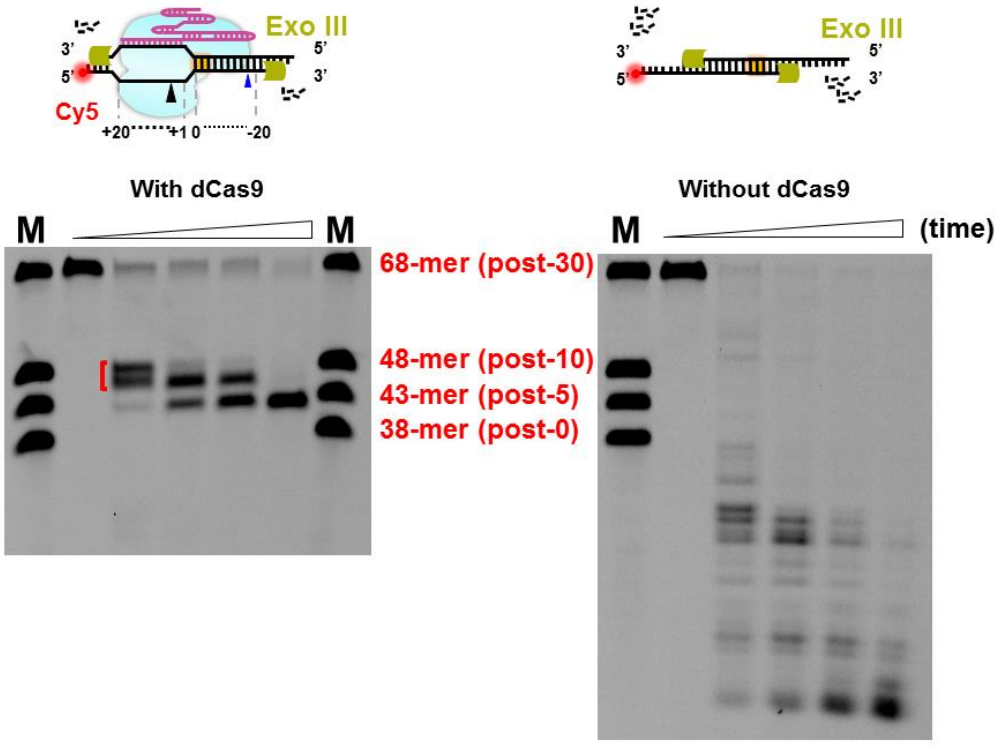

Fig. S4. Footprinting experiments with DNA bound by dCas9/sgRNA. To further confirm the existence of the post-PAM interaction detected in the DNA unzipping assay, we conduced exonuclease III footprinting experiments on target DNA with or without dCas9. Reactions were carried out as follows: After incubating dCas9/sgRNA complexes (300 nM) with ~1 nM DNA substrate for 30 minutes at 37 °C in reaction buffer, 100 units of exonuclease III (NEB) was added and reactions were incubated before quenching with formamide gel loading buffer supplemented with 50 mM EDTA. Reaction products were resolved by 15% denaturing polyacrylamide gel (7M urea PAGE) and visualized by phosphorimaging (GE Healthcare). The left panel showed a representative gel of footprinting of dCas9/sgRNA/DNA with Exo III. Reactions were quenched at five time points (0, 1, 2, 5, 10 min). The right panel showed a control exonuclease III footprinting experiment in the absence of dCas9. Interaction site between dCas9 and DNA near post-10 were detected after a short of period of incubation (1 min), resembling the post-PAM interaction detected in the reverse DNA unzipping assays.

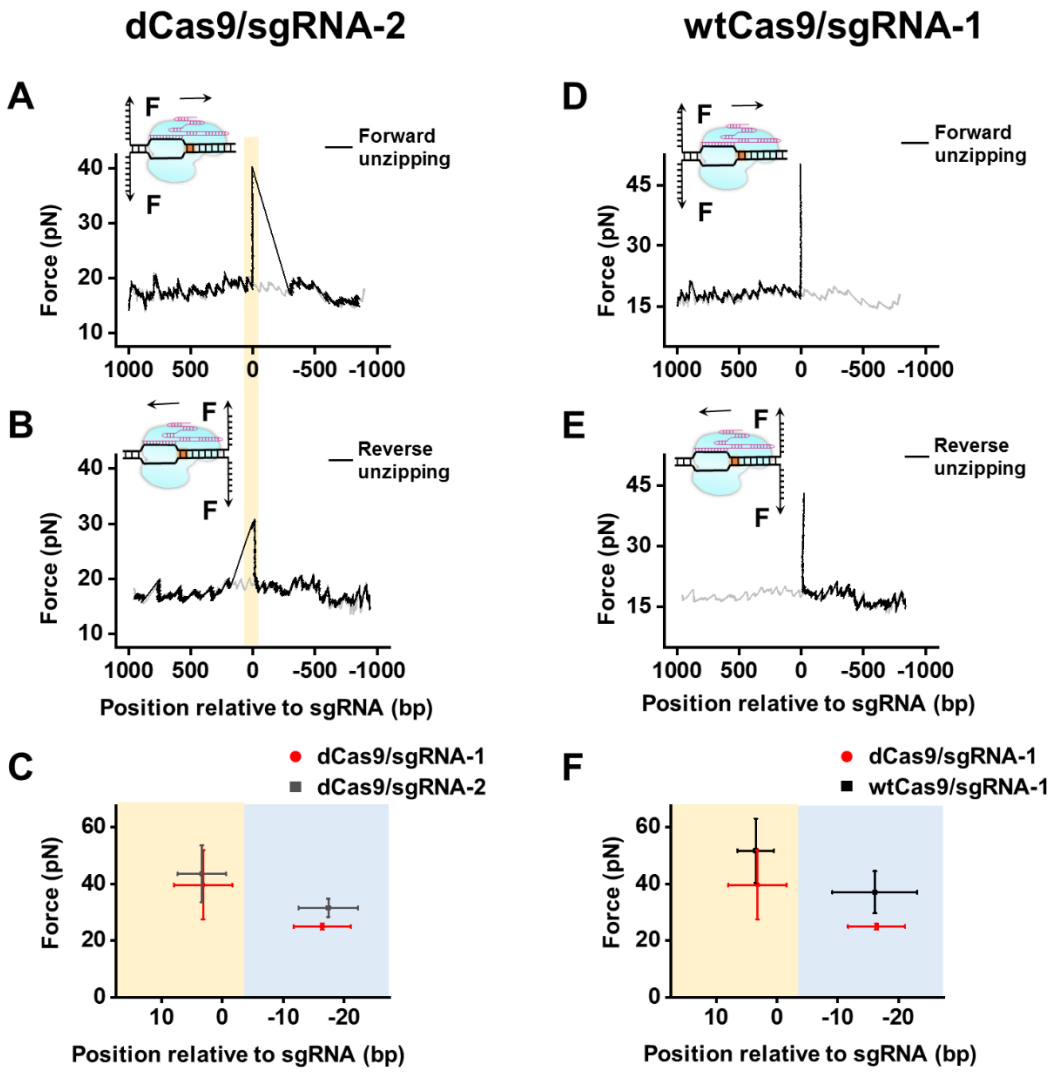

Fig. S5. Mapping of dCas9/sgRNA-2/DNA and wtCas9/sgRNA-1/DNA interactions. To examine whether the interactions of dCas9/sgRNA with DNA depend on the RNA-DNA complementary sequence, we designed a new sgRNA (named sgRNA-2, table S1) whose complementary DNA sequence locates at a different position on the trunk DNA (Methods). We conducted the forward (**A**) and reverse (**B**) unzipping experiments with this sgRNA-2 and dCas9. Two stable interactions were recorded, resembling those showed in Fig. 1. We next characterized the positions and strength of these two interactions and compared them with ones from sgRNA-1 (**C**). It turns out that the interaction positions are conserved, though the peak forces with sgRNA-2 are relatively higher than those with sgRNA-1. We also performed forward (**D**) and reverse (**E**) unzipping experiments with wtCas9 and 20 bp matched sgRNA to detect their interactions with on-target DNA. The unzipping force with Cas9-sgRNA immediately dropped to zero after the disruption of the interactions between wtCas9 and DNA due to Cas9's endonucleolytic cleavage. Other than that, the locations of interactions with wtCas9 are comparable with those from dCas9-sgRNA-1, although the disruption forces with wtCas9 are slighter higher than those with dCas9 (**F**).

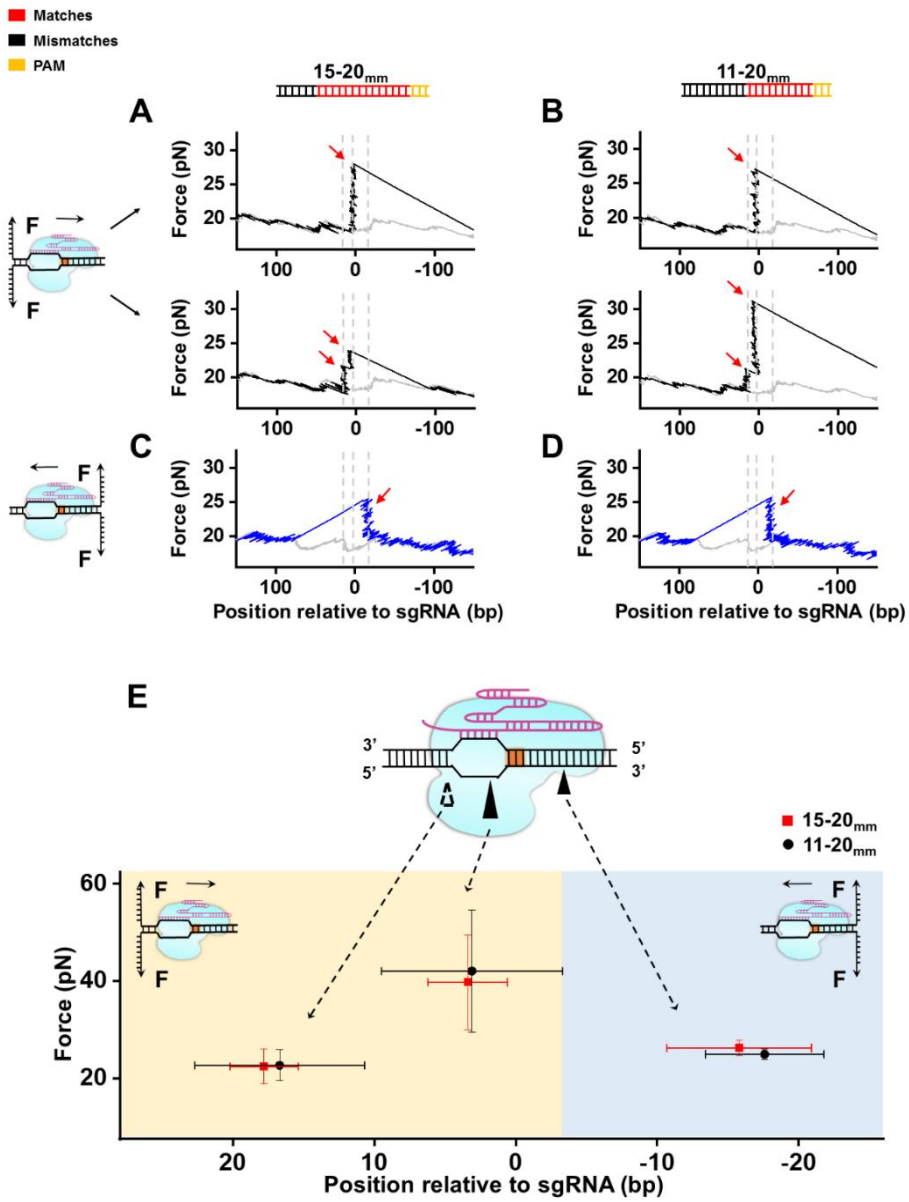

Fig. S6. Forward unzipping with R15-20$_{mm}$ and R11-20$_{mm}$ sgRNAs. We performed the forward unzipping experiments with R15-20$_{mm}$ (**A**) and R11-20$_{mm}$ (**B**) sgRNAs (table S1). Traces with one peak or dual peaks were observed in these experiments, which were similar to those with D15-20$_{mm}$ and D11-20$_{mm}$ templates (Fig. 2).

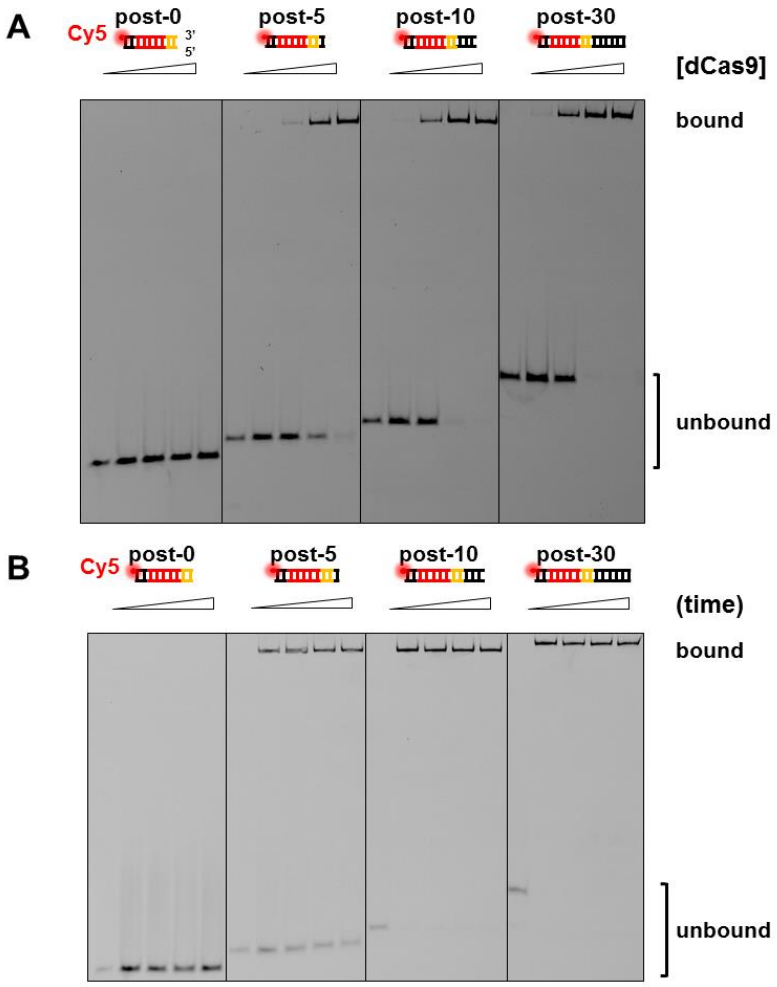

Fig. S7. EMSA confirmed the effect of the post-PAM DNA length on Cas9 binding. (**A**) A representative gel showing 1 nM DNA binding with dCas9 at various concentrations (0, 3, 30, 150, 300 nM). Reactions were quenched after 10 min incubation. (**B**) A representative gel showing 1nM of DNA binding with 300 nM of dCas9. Reactions were quenched at five time points (0, 1, 2, 5, 10 min). Samples were incubated at room temperature and resolved at 37 °C on an 8% native polyacrylamide gel. These sets of data clearly demonstrate that the binding affinity of dCas9 on DNA decreases when the post-PAM DNA length is shortened.

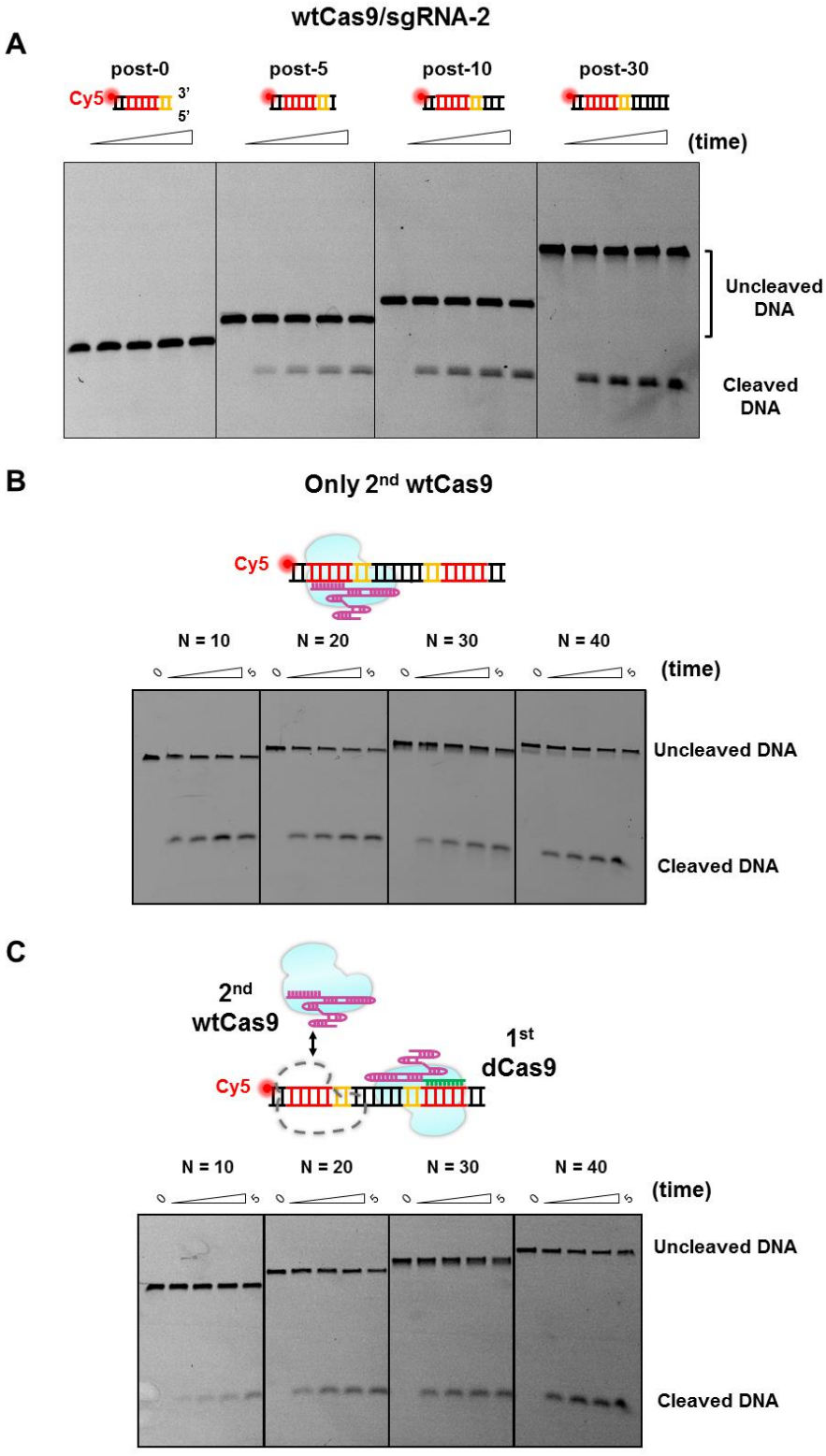

Fig. S8. DNA cleavage of wtCas9 with various DNA templates. (**A**) A representative gel showing wtCas9/sgRNA-2 cleavage with DNA templates containing various DNA lengths downstream of the PAM. Reactions were quenched at five time points (0, 5, 10, 15, 30 min). The cleavage efficiency of wtCas9 is apparently affected by the shortage of the DNA length downstream

of the PAM. (**B**, **C**) Representative gels of wtCas9 cleavage on PAM-in DNA templates with various DNA bases (N) between two PAMs in the absence (B) and presence (C) of the 1st dCas9. Reactions were quenched at five time points (0, 1, 2, 3, 5 min). Without the binding of the adjacent dCas9, wtCas9 showed similar cleavage efficiencies for these examined DNA templates (B). However, in contrast, in the presence of the 1st dCas9, the cleavage efficiencies of wtCas9 decreased as N decreased (C).

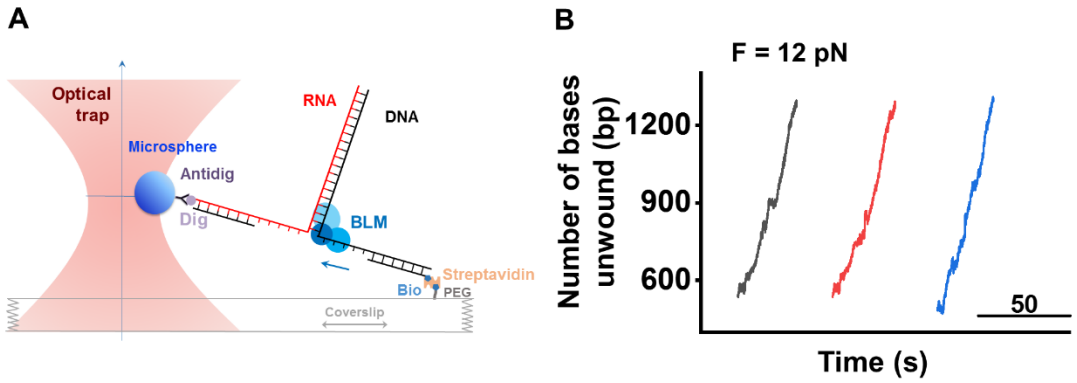

Fig. S9. BLM unwinding through DNA/RNA hybrid chain. (**A**) Schematic of BLM unwinding DNA/RNA hybrid chain using single-molecule optical-trap technique. (**B**) Representative traces of BLM unwinding DNA/RNA hybrid chain. After flowing 100 nM BLM into the chamber, we recorded the length of DNA-RNA hybrid tether under a constant force of 12 pN. No obvious long pauses were observed in this condition for BLM. We thus excluded the possibility that the observed pauses during BLM unwinding in the presence of pre-bound dCas9 was due to the BLM's inability to unwind RNA-DNA hybrid formed by sgRNA and the target DNA strand.

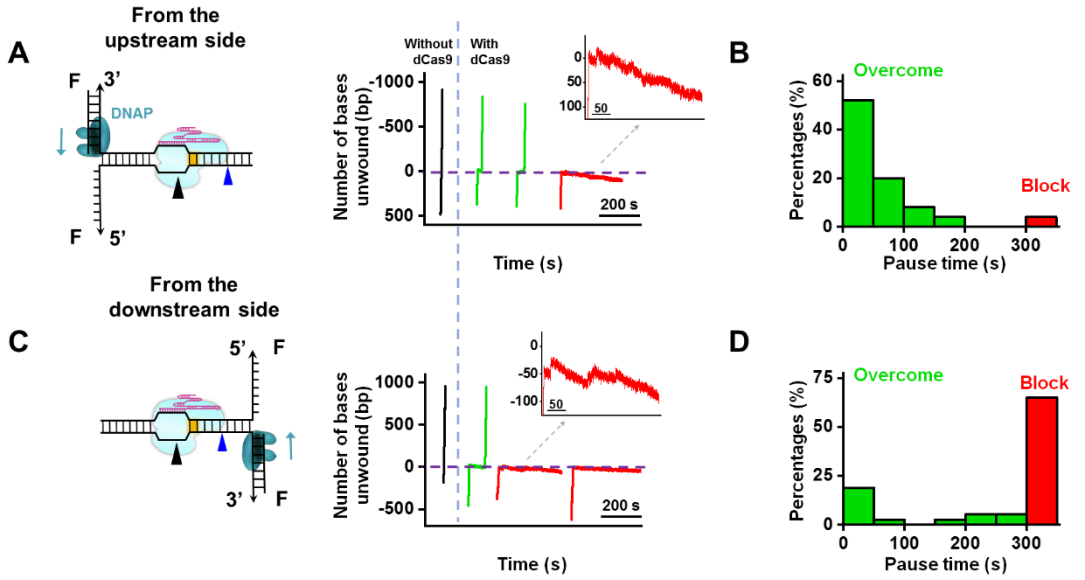

Fig. S10. Phi29 DNAP replicates through DNA-bound dCas9. The unwinding and replication of dsDNA by the Phi29 DNA polymerase (DNAP) was initiated either from the upstream (**A**) or downstream (**C**) side of the PAM. Representative traces showed the number of unwound base pairs versus time under an assisting force of 15 pN in the absence and presence of pre-bound dCas9. For clarity, traces have been shifted along the time axis. The dotted lines indicate the expected Cas9's binding position. Insets: zoom-in of the traces near the expected Cas9's binding position. (**B**, **D**) Histogram of Phi29 DNAP's pause time at the expected dCas9's binding position when unwinding initiated from the upstream (A) or downstream (C) side of the PAM. A fraction of DNAPs passed through the dCas9 (green) and the rest was blocked (red) in our experimental cutoff time (300 s). In this assay, Phi 29 DNAP-catalyzed unwinding and replicating of a fork junction were monitored as an increase in the DNA length under a constant force, which was not sufficient to mechanically unzip the fork junction. In the absence of dCas9, the Phi29 DNAP was found to processively unwind and replicate a forked DNA without apparent pauses under a force of 15 pN (A and C). We next repeated this experiment with a DNA template pre-bound by the dCas9 protein. We found that when Phi29 DNAPs encountered a dCas9 protein on the upstream side of the PAM, up to 88% of the DNAPs (n = 25), after a pause (~ 64 s) at the Cas9

binding site, displaced the bound protein and resumed the replication. The rest, however, was blocked within 5 minutes (experimental cutoff time, A and B). 40% of blocked traces near the Cas9 binding position showed an apparent decrease in DNA extension corresponding to a decrease in the number of base pairs replicated, most likely because of the exonuclease activity of the DNAP upon the collision. In contrast, when the Phi29 DNAP collided with the dCas9 protein on the downstream side of the PAM, only 35% of them (n = 37) replicated through the dCas9 protein and the rest of them was observed to be blocked for at least 5 minutes (C and D). In these blocked DNAPs, up to 81% of them showed backward movements upon the collision with the Cas9 protein (C).

SUPPLEMENTARY TABLES

Table S1. Sequences of sgRNAs and DNA.

For figures	Names	Sequences
Fig. 1-4, S2-4, S8, S10	sgRNA-1 (second in Fig. 3)	5'- **GGAGCGCACCAUCUUCUUCA**GUUUUAGAGCUAGAAAUAGCAAGUUAAAAUAAGGCUAGUCCGUUAUCAACUUGAA AAAGUGGCACCGAGUCGGUGCUUUUUUU
Fig. S5, S7, S8	sgRNA-2	5'- GG**CUCGUGACCACCCUGACCUA**GUUUUAGAGCUAGAAAUAGCAAGUUAAAAUAAGGCUAGUCCGUUAUCAACUUG AAAAAGUGGCACCGAGUCGGUGCUUUUUUU
Fig. 3, S8	SgRNA-3 (first)	5'-GG**CAAGUCCGCCAUGCCCGA**GUUUUAGAGCUAGAAAUAGCAAGUUAAAAUAAGGCUAGUCCGUUAUCAACUUGAA AAAGUGGCACCGAGUCGGUGCUUUUUUU
Fig. S6	sgRNA R15-20$_{mm}$	5'-GG**AAGAUA**CACCAUCUUCUUCAGUUUUAGAGCUAGAAAUAGCAAGUUAAAAUAAGGCUAGUCCGUUAUCAACUUG AAAAAGUGGCACCGAGUCGGUGCUUUUUUU
Fig. S6	sgRNA R11-20$_{mm}$	5'-GG**AAGAUAUGUU**AUCUUCUUCAGUUUUAGAGCUAGAAAUAGCAAGUUAAAAUAAGGCUAGUCCGUUAUCAACUUG AAAAAGUGGCACCGAGUCGGUGCUUUUUUU
Fig. 1, 3-4, S2-4, S6, S8, S10	DNA binding site-1	5'–…GGAGCGCACCATCTTCTTCAAGG…-3' 3'–…**CCTCGCGTGGTAGAAGAAGT**TCC…-5'
Fig. 2	DNA binding site-2 (D15-20$_{mm}$)	5'–…CCTCGCCACCATCTTCTTCAAGG…-3' 3'–…**GGAGCG****GTGGTAGAAGAAGT**TCC…-5'
Fig. 2	DNA binding site-3 (D11-20$_{mm}$)	5'–…CCTCGCGTGGATCTTCTTCAAGG…-3' 3'–…**GGAGCGCACC****TAGAAGAAGT**TCC…-5'
Fig. 3, S8	DNA binding sith-4	5'-…GGCAAGTCCGCCATGCCCGAAGG…-3' 3'-…**CCGTTCAGGCGGTACGGGCT**TCC…-5'
Fig. S5, S7, S8	DNA binding site-5	5'-…CTCGTGACCACCCTGACCTACGG…-3' 3'-…**GAGCACTGGTGGGACTGGAT**GCC…-5'

The protospacer sequences in sgRNAs are in bold with matched sequences in red and mismatched sequences in blue. PAM sequences are highlighted in yellow.

Table S2. Sequences of oligos used for bulk DNA cleavage assays.

Object	Sequences for bulk cleavage assays
Cy5-post-0	5'- Cy5-CGAAGGCTACGTCCAGGAGCGCACCATCTTCTTCAAGG -3' 3'- GCTTCCGATGCAGGTCCTCGCGTGGTAGAAGAAGTTCC -5'
Cy5-post-5	5'- Cy5-CGAAGGCTACGTCCAGGAGCGCACCATCTTCTTCAAGGACGAC -3' 3'- GCTTCCGATGCAGGTCCTCGCGTGGTAGAAGAAGTTCCTGCTG -5'
Cy5-post-10	5'- Cy5-CGAAGGCTACGTCCAGGAGCGCACCATCTTCTTCAAGGACGACGGCAA -3' 3'- GCTTCCGATGCAGGTCCTCGCGTGGTAGAAGAAGTTCCTGCTGCCGTT -5'
Cy5-post-30	5'- Cy5-CGAAGGCTACGTCCAGGAGCGCACCATCTTCTTCAAGGACGACGGCAACTACAAGACCCGCGCCGAGG -3' 3'- GCTTCCGATGCAGGTCCTCGCGTGGTAGAAGAAGTTCCTGCTGCCGTTGATGTTCTGGGCGCGGCTCC -5'
Cy5-post-0-new	5'- Cy5-GTGCCCTGGCCCACCCTCGTGACCACCCTGACCTACGG -3' 3'- CACGGGACCGGGTGGGAGCACTGGTGGGACTGGATGCC -5'
Cy5-post-5-new	5'- Cy5- GTGCCCTGGCCCACCCTCGTGACCACCCTGACCTACGGCGTGC -3' 3'- CACGGGACCGGGTGGGAGCACTGGTGGGACTGGATGCCGCACG -5'
Cy5-post-10-new	5'- Cy5- GTGCCCTGGCCCACCCTCGTGACCACCCTGACCTACGGCGTGCAGTGC -3' 3'- CACGGGACCGGGTGGGAGCACTGGTGGGACTGGATGCCGCACGTCACG -5'
Cy5-post-30-new	5'- Cy5- GTGCCCTGGCCCACCCTCGTGACCACCCTGACCTACGGCGTGCAGTGCTTCAGCCGCTACCCCGACCA -3' 3'- CACGGGACCGGGTGGGAGCACTGGTGGGACTGGATGCCGCACGTCACGAAGTCGGCGATGGGGCTGGT-5'
PAM-in (N = 10)	5'- Cy5-CGTCCAGGAGCGCACCATCTTCTTCAAGGACGACGGCAACCTTCGGGCATGGCGGACTTGCCATCAGC -3' 3'- GCAGGTCCTCGCGTGGTAGAAGAAGTTCCTGCTGCCGTTGGAAGCCCGTACCGCCTGAACGGTAGTCG -5'
PAM-in (N = 20)	5'- Cy5-CGTCCAGGAGCGCACCATCTTCTTCAAGGACGACGGCAACTACAAGACCCCTTCGGGCATGGCGGACTTGCCATCAGC -3' 3'- GCAGGTCCTCGCGTGGTAGAAGAAGTTCCTGCTGCCGTTGATGTTCTGGGGAAGCCCGTACCGCCTGAACGGTAGTCG -5'
PAM-in (N = 30)	5'- Cy5-CGTCCAGGAGCGCACCATCTTCTTCAAGGACGACGGCAACTACAAGACCCGCGCCGAGGCCTTCGGGCATGGCGGACTTGCCATCAGC -3' 3'- GCAGGTCCTCGCGTGGTAGAAGAAGTTCCTGCTGCCGTTGATGTTCTGGGCGCGGCTCCGGAAGCCCGTACCGCCTGAACGGTAGTCG -5'
PAM-in (N = 40)	5'- Cy5-CGTCCAGGAGCGCACCATCTTCTTCAAGGACGACGGCAACTACAAGACCCGCGCCGAGGTGAAGTTCGACCTTCGGGCATGGCGGACTTGCCATCAGC -3' 3'- GCAGGTCCTCGCGTGGTAGAAGAAGTTCCTGCTGCCGTTGATGTTCTGGGCGCGGCTCCTCTTCAAGCTGGAAGCCCGTACCGCCTGAACGGTAGTCG -5'

PAM sequences are highlighted in yellow. On-target DNA sequences are in red and marked with underline.